

Ion-induced kinetic electron emission from HOPG with different surface orientation

S. CERNUSCA, M. FÜRSATZ, HP. WINTER and F. AUMAYR(*)

*Institut für Allgemeine Physik, TU Wien
Wiedner Haupstr. 8, A-1040 Vienna, Austria*

received 21 December 2004; accepted in final form 18 April 2005

published online 11 May 2005

PACS. 34.50.Dy – Interactions of atoms and molecules with surfaces; photon and electron emission; neutralization of ions.

PACS. 79.20.Rf – Atomic, molecular, and ion beam impact and interactions with surfaces.

Abstract. – Total electron emission yields for impact of H^+ , H_2^+ , C^+ , N^+ , O^+ and Ar^+ ions (impact energy 2–10 keV) on clean highly oriented pyrolytic graphite (HOPG) have been measured. An enhancement in the electron yield of more than a factor of 2 is found when comparing results for differently oriented HOPG surfaces (orientation of the graphite layers with respect to the surface). By analyzing these data we elucidate the influence of electron transport on kinetic electron emission and derive direction-dependent mean escape depths for low-energy electrons.

Electron emission is a fundamental phenomenon in slow ion - surface interaction and intimately connected to projectile energy deposition in the target [1–7]. It is also of importance for many applications like electrical discharges, plasma-wall interaction, surface analysis and single-particle detection. More recent interest in particle-induced electron emission is due to its key role in plasma display panels, where it effects the firing and sustaining voltage and therefore the power consumption of the panels [8], and for spacecraft charging as the cause of many system anomalies and component failures [9].

Although electron emission from solid surfaces due to the impact of energetic ions (*i.e.* kinetic electron emission, KE) is a well-investigated process, most studies on KE so far have focused on the primary mechanism of exciting electrons within the target surface. However, before escaping into vacuum the electrons have to propagate towards the surface. Therefore, electron transport has a significant influence on the resulting total KE yield [1,4]. For example, it is commonly assumed that the mean free path of low-energy electrons is larger in insulators than in metals, which increases their escape depth and the total electron yield [3]. However, KE from insulating and conducting surfaces is caused by different mechanisms, and it is therefore difficult to separate the role of electron transport from the primary excitation mechanism. For projectiles grazingly scattered from a single-crystal target electron emission is found to depend on the azimuthal settings of the target surface [3]. Possible explanations include either a change in the escape depth of electrons or different penetration depths of the projectiles.

(*) E-mail: aumayr@iap.tuwien.ac.at

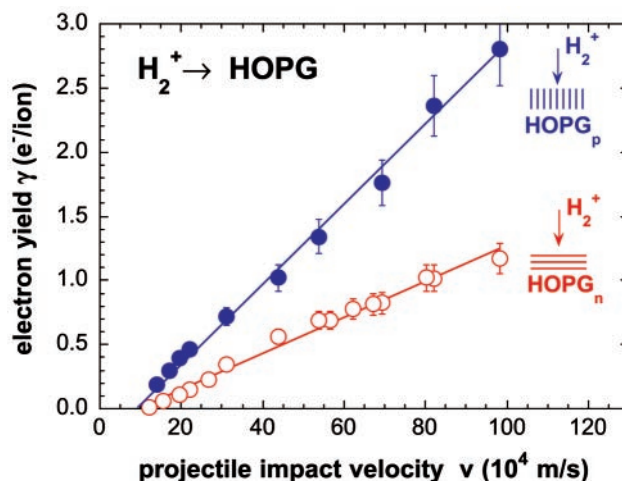


Fig. 1 – Measured total electron emission yields for impact of H_2^+ ions on differently oriented HOPG surfaces (open circles: HOPG_n , full circles: HOPG_p ; the orientation of graphite layers is indicated by the inserts).

Highly oriented pyrolytic graphite (HOPG) is a standard target used in surface physics, easy to clean and handle. It consists of well-defined layered carbon sheets which exhibit large differences in electrical and thermal conductivity parallel to these layers (high conductivity) as compared to the perpendicular direction (low conductivity). Since electron transport in a conductor is related to electrical conductivity, the dependence of the electron emission yield on the orientation of the layers relative to the surface would allow us to study the role of electron transport in KE separated from the primary excitation mechanism.

We have therefore studied electron emission yields induced by normal impact of singly charged ions (H^+ , H_2^+ , C^+ , N^+ , O^+ and Ar^+ , impact energy between 2 and 10 keV) on clean HOPG of two different orientations. Thermal and electrical conductivities of the here used HOPG target (tectura [10], size: $12 \times 12 \times 8$ mm) are by one to two orders of magnitude higher along the graphite layers than perpendicular to them. In the following “ HOPG_n ” refers to a target where the graphite layers are oriented normal to the incident beam direction (and thus parallel to the surface plane) while “ HOPG_p ” refers to a target with the graphite layers oriented parallel to the incident beam direction (and thus normal to the surface plane, cf. insert in fig. 1).

The contribution by potential electron emission to the total electron yields was in all cases of no relevance [1, 5, 6]. Experimental methods for KE measurements were the same as in our earlier investigations with atomically clean polycrystalline gold and HOPG [11], *i.e.* the total electron yield γ was obtained from the currents of impinging ions and emitted electrons measured for different target bias. Both targets were prepared by cleaving the surface with an adhesive tape just before transfer into vacuum. Measurements were carried out under UHV conditions (typically 10^{-10} mbar). To obtain reproducible results, surface contaminants had to be removed first. This was achieved by sputter-cleaning via impact of 5 keV Ar^{2+} ions (ion dose below 10^{15} ions/cm²). During sputter-cleaning, the “apparent” electron emission yield was monitored and the sputter cleaning terminated as soon as a constant value was reached. A certain deterioration of the surface flatness has to be expected due to this necessary procedure.

An enhancement in the electron yield by up to a factor of 2.3 is found when comparing

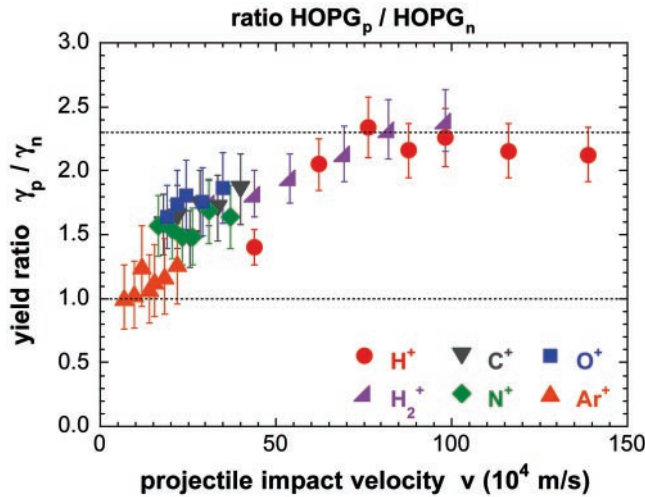


Fig. 2 – Ratios of electron yields for impact of singly charged ions on HOPG_p and HOPG_n (γ_p/γ_n) as a function of projectile impact velocity.

results for differently oriented HOPG surfaces. As an example, we show results for impact of H₂⁺ ions on HOPG_p and HOPG_n, respectively, in fig. 1.

From these data for H₂⁺ and similar data for other projectile ions (H⁺, C⁺, N⁺, O⁺ and Ar⁺) we note the following general trends:

- i) In all cases, the measured electron yields increase more or less linearly with projectile velocity.
- ii) The apparent threshold velocity (extrapolation to zero yield) differs slightly from projectile to projectile (heavier projectiles exhibit a comparably lower threshold, see discussion in [11]), but for a given projectile ion the threshold does not significantly depend on target orientation (within our experimental errors).
- iii) For all impact velocities the KE yields are higher for HOPG_p than for HOPG_n. For heavier projectiles the enhancement (ratio of electron yields γ_p/γ_n) is smaller and approaches unity for very slow Ar⁺ projectiles.

Figure 2 summarizes our results by showing ratios of electron yields γ_p/γ_n for impact of various singly charged ions on HOPG_p and HOPG_n as a function of projectile impact velocity.

At first sight, the observed behaviour can be explained by assuming that electron transport along the graphite layers (*i.e.* towards the surface for HOPG_p orientation) is enhanced in comparison with electron transport across (perpendicular to) the HOPG layers. An enhanced electron transport means that the mean escape depth (“attenuation length”) for low-energy electrons λ is larger for HOPG_p than for HOPG_n, *i.e.* $\lambda_p > \lambda_n$, so electrons originating from deeper inside the solid are able to reach the surface, which results in a higher electron emission yield. As long as the projectile ion range R exceeds the mean electron escape depth (*i.e.* for fast projectiles), the observed yield ratio γ_p/γ_n just reflects the ratio of the mean escape depths λ_p/λ_n . Very slow projectiles, however, can penetrate a few atomic layers only. In this case, the projectile range R is comparable to or even less than λ , and the electrons will therefore have similar probabilities to escape from the differently oriented HOPG surfaces, for which case the yield ratio approaches unity.

Before developing a more quantitative model, let us consider (and exclude) some other possible explanations for the observed yield differences.

1) *Different electron production mechanisms and/or target work functions*: The principal excitation mechanisms for kinetic electron emission involve binary collisions of the projectile with quasi-free target electrons, and electron promotion during projectile collisions with the target atom cores [1,5]. While the first KE mechanism is typical for light projectiles impinging onto conducting surfaces [1,12], the second one contributes to electron emission from metals for heavier projectiles [1,7] and will be the main source of electrons for insulator targets [1,3,5,13]. Both mechanisms are not expected to depend on the orientation of the HOPG layers (possible channeling effects will be discussed below). On the contrary, our data indicate that identical primary excitation mechanism(s) are at work, since measured threshold velocities do not depend on the target orientation (see fig. 1). This observation can also be used to exclude differences in work function for HOPG_p and HOPG_n as a possible source for the observed enhancement. The KE threshold reflects the minimum energy necessary to excite electrons above the vacuum level and therefore also depends on the work function W_ϕ . When assuming a free-electron gas target surface (Fermi energy E_F and velocity v_F) the threshold velocity v_{th} is determined from the minimum momentum transfer in binary collisions of projectiles with free electrons to overcome the surface work function W_ϕ [1,5,14]

$$v_{th} = \frac{1}{2} \cdot v_F \cdot \left(\sqrt{1 + \frac{W_\phi}{E_F}} - 1 \right). \quad (1)$$

For HOPG as a target, this simple model yields a threshold value of $v_{th} \approx 1.5 \times 10^5$ m/s [11], which is close to the observed threshold for light projectile ions (cf. fig. 1). A large change in work function as would be required to explain a doubling of the electron emission yields would certainly also lead to considerably different threshold velocities.

2) *Channeling effects* for ions traveling parallel to the graphite layers (HOPG_p) could result in an increased ion range. Since channeled projectiles would deposit their energy deeper inside the target, however, we would expect a smaller electron emission yield for HOPG_p than for HOPG_n, in contrast to our observations.

3) *Surface roughness* can have an important influence on total electron emission yield. For a perfectly flat surface one would expect a considerable increase of the yield when changing from normal ion impact ($\theta = 90^\circ$ with respect to the surface plane) to an inclined impact direction (according to [1] with about $1/\sin(\theta)$). For a rough surface, the microscopic impact angles are statistically distributed around average values $\theta < 90^\circ$ (even at “nominal” normal incidence). The yield for perpendicular impact on a rough surface might therefore be larger than for a flat one. On the other hand, carbon black (carbon soot) is often used as an electron absorber because of its extraordinary low secondary-electron yield. Here self-absorption in the rough surface is expected to reduce electron emission significantly. It was our main concern that cleaving with an adhesive tape, although known to produce flat surfaces for HOPG_n, could make a quite rough HOPG_p surface. To check this point, we have measured the electron emission yield for both target orientations as a function of ion impact angle θ (fig. 3). Within experimental errors both data sets exhibit a $\sin^{-1}(\theta)$ -dependence as long as the impact angles become not too small. Our results indicate that the used HOPG_p and HOPG_n surfaces are of comparable roughness, which is probably a result of the sputter-cleaning with Ar ions. Surface roughness could therefore not account for the large yield differences observed in our experiments.

For a quantitative analysis of the data along the lines of our transport hypothesis we have plotted the measured yield ratios γ_p/γ_n as a function of projected ion range in fig. 4. The

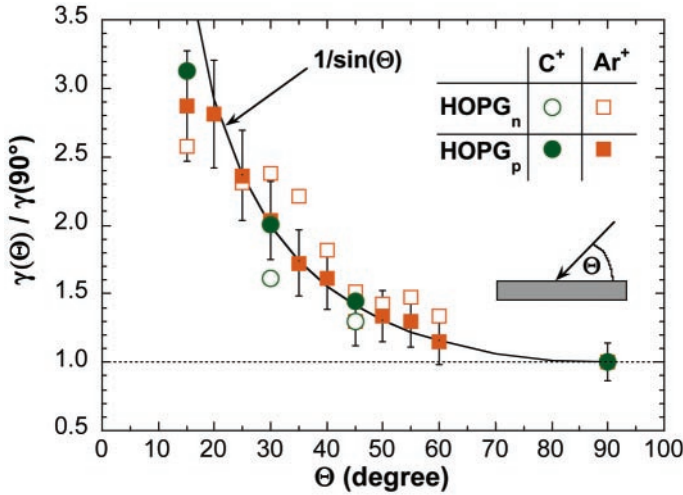


Fig. 3 – Dependence of the electron emission yields from both targets on the ion impact angle θ . The data points (open symbols for HOPG_n, full symbols for HOPG_p) were fitted with a $1/\sin\theta$ dependence.

latter have been calculated with the SRIM 2003 code (*i.e.* the most recent version of the TRIM code [15]). In a simple model we then assume that electron production dy in a layer $x, x + dx$ below the surface is proportional to the stopping power dE/dx [14, 16], which in the impact energy regime considered here increases linearly with projectile velocity v :

$$dy = y(x) \cdot dx \propto \left| \frac{dE}{dx}(x) \right| \cdot dx \propto v(x) \cdot dx. \tag{2}$$

Assuming further an exponentially decreasing probability for electrons to reach the surface [1,

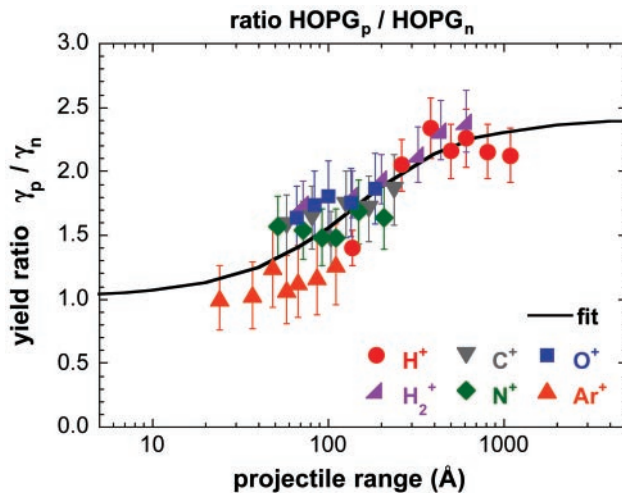


Fig. 4 – Ratios of electron yields λ_p/λ_n from fig. 2 plotted as a function of projectile range (as calculated by using SRIM-2003 [11]). Experimental data were fitted according to eq. (4).

2] from a mean escape depth λ , the total electron yield γ is derived from

$$\gamma = \int_0^R y(x) \cdot e^{-x/\lambda} \cdot dx \propto \lambda^2 \left[\frac{R}{\lambda} + e^{-R/\lambda} - 1 \right]. \quad (3)$$

For different escape depths for HOPG_p and HOPG_n ($\lambda_p \neq \lambda_n$) the corresponding yield ratios as a function of projectile range R are given by

$$\frac{\gamma_p}{\gamma_n}(R) = \frac{\lambda_p^2 \left[\frac{R}{\lambda_p} + e^{-R/\lambda_p} - 1 \right]}{\lambda_n^2 \left[\frac{R}{\lambda_n} + e^{-R/\lambda_n} - 1 \right]}. \quad (4)$$

In two limiting cases (projectile range much larger or much smaller than both mean escape depths) eq. (4) simplifies to

$$\begin{aligned} R \gg \lambda_n, \lambda_p &\implies \frac{\gamma_p}{\gamma_n} \longrightarrow \frac{\lambda_p}{\lambda_n}, \\ R \ll \lambda_n, \lambda_p &\implies \frac{\gamma_p}{\gamma_n} \longrightarrow 1. \end{aligned} \quad (5)$$

In fig. 4 we have fitted our experimental data with this model (eq. (4)). Despite its simplicity, there is quite satisfactory agreement with the experimental results. As fit values we obtain as estimates for the mean escape depths of low-energy electrons $\lambda_n \approx 30 \text{ \AA}$ and $\lambda_p \approx 73 \text{ \AA}$. These values are consistent with data from the literature which for electron energies below 10 eV involve mean attenuation lengths between 10 and 100 \AA for various materials [17].

In summary, we have found that kinetic electron emission from HOPG caused by the impact of various singly charged ions depends on the orientation of graphite layers with respect to the target surface. We can rule out other conceivable reasons for this difference and explain it by a comparably enhanced electron transport along the graphite layers. By analyzing our data within a simple transport model we are able to isolate the effect of electron transport on kinetic electron emission and to derive mean escape depths for low-energy electrons.

This work was carried out within Association EURATOM-OEAW and has been supported by Kommission zur Koordination der Kernfusionsforschung in Österreich and Austrian Fonds zur Förderung der wissenschaftlichen Forschung (FWF). The authors acknowledge valuable discussions with Profs. J. BURGDÖRFER and W. WERNER (both at TU Wien).

REFERENCES

- [1] HASSELKAMP D., in *Particle Induced Electron Emission II*, Vol. **123**, edited by HÖHLER G. (Springer, Heidelberg) 1992, p. 1.
- [2] SIGMUND P. and TOUGAARD S., in *Inelastic Particle-Surface Collisions*, edited by TAGLAUER E. and HEILAND W. (Springer, Berlin) 1981, p. 2.
- [3] SCHOU J., *Scan. Micr.*, **2** (1988) 607; SCHOU J., in *Ionization of Solids by Heavy Particles*, Vol. **306**, edited by BARAGIOLA R. (Plenum, New York) 1993, p. 351; BENAZETH N., *Nucl. Instrum. Methods Phys. Res.*, **194** (1982) 405.
- [4] RÖSLER M. and BRAUER W., in *Particle Induced Electron Emission I*, Vol. **122**, edited by HÖHLER G. (Springer, Berlin) 1991.

- [5] BARAGIOLA R., in *Low Energy Ion-Surface Interactions*, edited by RABALAIS J. W. (Wiley) 1993, Chapt. IV.
- [6] ARNAU A. *et al.*, *Surf. Sci. Rep.*, **229** (1997) 1.
- [7] WINTER H., *Phys. Rep.*, **367** (2002) 387.
- [8] BOEUF J. P., *J. Phys. D*, **36** (2003) R53.
- [9] FROONINCKX T. B. and SOJKA J. J., *J. Geophys. Res.*, **97** (1992) 2985; LEACH R. D. and ALEXANDER M. D., *Failures and Anomalies attributed to Spacecraft Charging*, NASA **RP-1375**, Marshall Space Flight Center (1995); BILÉN S. G., AGÜERO V. M., GILCHRIST B. E. and RAITT W. J., *J. Spacecraft Rockets*, **34** (1997) 655.
- [10] Tectra GmbH, www.tectra.de.
- [11] CERNUSCA S., DIEM A., WINTER HP., AUMAYR F., LÖRINCIK J. and SROUBEK Z., *Nucl. Instrum. Methods Phys. Res. B*, **193** (2002) 616.
- [12] LEDERER S., MAASS K., BLAETH D., WINTER H., WINTER HP. and AUMAYR F., *Phys. Rev. B*, **67** (2003) 121405(R).
- [13] MERTENS A., LEDERER S., MAASS K., WINTER H., STÖCKL J., WINTER HP. and AUMAYR F., *Phys. Rev. B*, **65** (2002) 132410.
- [14] BARAGIOLA R. A., ALONSO E. V. and OLIVA-FLORIO A., *Phys. Rev. B*, **19** (1979) 121.
- [15] ZIEGLER J. F., BIRSACK J. P. and LITTMARK U., *The Stopping and Range of Ions in Matter* (Pergamon, New York) 1985. The SRIM2003 code can be downloaded from <http://www.srim.org>.
- [16] BEUHLER R. J. and FRIEDMAN L., *J. Appl. Phys.*, **48** (1977) 3928.
- [17] SEAH M. P. and DENCH W. A., *Surf. Interf. Anal.*, **2** (1980) 53; PENN D. R., *Phys. Rev. B*, **13** (1976) 5248; TANUMA S., POWELL C. J. and PENN D. R., *J. Vac. Sci. Technol. A*, **8** (1990) 2213; ZANGWILL A., *Physics at Surfaces* (Cambridge University Press) 1988.